Proceedings of Ninth World Conference on Earthquake Engineering
August 2-9, 1988, Tokyo-Kyoto, JAPAN (Vol.IV)

6-7-10

EXPERIMENTAL INVESTIGATION ON THE SEISMIC PERFORMANCE OF PRECAST WALLS

Peter Mueller[1]

[1] Fritz Engineering Laboratory, Lehigh University
Bethlehem, Pennsylvania, USA

SUMMARY

This paper briefly reviews results from tests on the behavior of precast walls typical of U.S. large panel building construction that were subjected to cyclic seismic and constant axial load. The walls exhibit a completely altered shear transfer mechanism and a significant concentration of elastic and inelastic deformations into the connections. Compared to cast-in-place walls, this results in increased local ductility demands (particularly near the base connection) or, conversely, in a reduced overall ductility capacity. Providing boundary elements near the base connection is very effective, doubling the ductility. The behavioral differences to monolithic walls clearly establish the need for code provisions that specifically address precast walls.

INTRODUCTION

Current seismic codes in the USA do not specifically address precast concrete. Precast concrete is permitted, if it satisfies the requirements for monolithic, cast-in-place concrete. The general objective of this experimental research program was to determine the seismic performance of precast walls which do not necessarily satisfy these requirements and are detailed for ease of fabrication and erection according to current practice in zones of low to intermediate seismicity. The specific objectives were to investigate the two main concerns, namely: (1) the effect of horizontal connections on ductility and energy dissipation capacity, and (2) their effect on shear transfer mechanism and capacity.

TEST SPECIMEN AND PROCEDURE

Five 20 ft. (6m) high and 8 ft. (2.4m) long wall specimens were tested (Ref. 1 to 3) which represent scaled-down models of the lower half of a ten-story precast wall with details typical of large panel building construction in the USA. Story-sized wall panels and hollow-core floor plank stubs were stacked on top of each other and connected with platform-type horizontal connections (Fig. 1) except for the base connection which did not contain floor planks. The parameter variation includes two reinforcement ratios, 0.33% (corresponding to ACI minimum reinforcement) and 0.17%; two axial force nominal stress levels, 550 psi (3.8 MPa) and 350 psi (2.4 MPa); and prestress/no prestress. The low-high combination (PW1) and the high-low combination (PW2) achieve in different ways the same lateral strength but PW2 is at the critical limit for shear slip. The high-high combination (PW3) probes a diagonal crushing failure mode of the horizontal connection. PW4 and PW5 are the prestressed companion specimens for the non-prestressed walls PW3 and PW2, respectively. The vertical continuity steel was connected with grouted splice sleeves in the three non-prestressed walls and with post-tensioning bar couplers in the two prestressed walls. The walls were subjected to a constant axial load and a predetermined sequence of lateral displacement cycles of increasing amplitude. The walls were extensively instrumented.

TEST RESULTS

The following brief review of the test results centers on the effect that the horizontal connections have on (1) shear transfer mechanisms and shear strength, and (2) energy dissipation and ductility.

Shear Transfer in Panels Regarding (1) two aspects must be clearly distinguished: (i) shear transfer mechanism and strength of the connections and (ii) the effect that (i) has on the shear transfer mechanism and strength of the panels. This section addresses the latter aspect. The crack pattern developed in these precast walls (Ref. 1 to 3) is quite different from that in monolithic walls and reflects a significantly altered shear transfer mechanism. The dominating and most wide cracks in the non-prestressed walls and the only cracks in the prestressed walls are steeply inclined (shear) cracks which, however, never penetrate into the lower panel as if the lower panel edge were in transverse compression. Indeed, if the connections open up in the tension zone, shear can only be transferred over the closed compression zone and the panels act as horizontal cantilevers, their fixed end being encased in the wall compression zone and developing flexure-shear cracks and their tip being loaded by the differential tension from the wall flexural reinforcement. In effect, these precast walls represent an ideal realization of Kani´s shear teeth model! From an alternative perspective, the compression diagonals of the truss model shown in Fig. 2 must "bypass" the open connections and are forced into the panel diagonals. From both perspectives, horizontal reinforcement is most effectively placed along the top edge of the panel and was determined from the truss model. In spite of the fact that a significant percentage of the shear could be assigned to the inclined compression chord (a rationally determined V_c estimate!), twice as much shear reinforcement was required as for a similar monolithic wall and indeed needed, since strain gage readings did indicate yield strains. Since the spacing of the connections is much closer than the distance d (depth) over which local stress disturbances usually decay in a beam, these precast walls consist entirely of so-called D(isturbed) regions for which beam theory does not necessarily hold. This was evident not only from the point of view of shear but also flexure in the sense that plane sections did not remain plain in connections due to the "cantilever bending" effect. Of course, these precast walls could be designed to behave more similarly to monolithic walls by providing shear keys or connectors. While the present design eases fabrication and erection, it must be realized from a structural point of view that it is precisely the capacity of the omitted shear keys or connectors in the connections that has to be made up for in the panels in the form of the (increased) horizontal edge reinforcement. Nothing comes gratis in life!

Shear Strength and Slip of Platform Connection Due to the smooth panel edges and the lack of shear connectors, shear transfer over the connection interface occurs primarily through friction. Hence, shear resistance is given by friction coefficient times concrete compressive resultant which equals the axial load if both compressive and tensile steel are yielding and strain hardening is neglected. Specimen PW2 was designed to probe shear slip and with a shear-axial force ratio of 0.55 did develop 0.8in (20mm) slip in the first platform connection as illustrated in Fig. 3, suggesting an apparent friction coefficient of $\mu = 0.55$. Since the higher-up connections did not slip although the compressive resultant tends to decrease with decreasing moment and the shear force was the same, μ must increase with decreasing stress levels. This has indeed been observed in many other tests. PW5, similar to PW2 except that it is prestressed, did not slip due to the prestress and possibly due to interlock with anchor hardware in the connection and smaller strain hardening. All other specimens had lower shear-axial force ratios and did not slip. The large slip resulted in severe spalling of the cover down to the wire mesh cage in panel corners, pointing out its importance, and started to tear apart the floor planks, jeopardizing anchorage of the structural integrity reinforcement between planks. In spite of all that the connection showed no signs of failure and behaved unexpectedly ductile in flexure as illustrated in Fig. 4. Failure of PW2 occurred in the lower base connection due to bond loss in the splice sleeves. Neither did the first platform connection of PW3, the most highly stressed both in flexure and shear, ever show any signs of distress.

<u>Inelastic Deformation Capacity and Ductility</u> of these precast walls are most significantly affected by a severe concentration of both elastic and inelastic deformations into connections (particularly the base connection) because of their reduced stiffness and strength. The ensuing relatively increased local ductility demands in the connection areas result in a lower global ductility capacity relative to cast-in-place walls. Because of the severe opening of the base connection the corners of the bottom panel are particularly severely strained. Therefore spiral reinforcement dropped over splice sleeves or PT-ducts and extending over half the panel height, proved very effective, doubling the top deflection ductility ration. Compared to their effect, the effects of the other parameters proved irrelevant. The spirals prevent the premature splitting and crushing of the panel and the ensuing inelastic buckling of the rebar/splice sleeve assembly that was observed in PW1 which didn´t have them, and act as confining boundary elements. PW2, also without spirals, ultimately failed through loss of bond in the splice sleeves due to strain-hardening beyond their capacity (90 ksi!). Because some resistance was retained, this is probably preferable to the alternative: rupturing of the bar. Both reached 3 times the nominal first yield displacement (DY). PW3, PW4, and PW5, all with spirals, reached 6 DY in spite of severe distress of the compression corners, and final failure occurred on the tension side: loss of bond in the splice sleeves (PW3), rupturing of PT-bar (PW4) and a premature weld failure at a base block coupler (PW5).

Figs. 5 to 10 compare the behavior of the non-prestressed and prestressed companion specimens PW3 and PW4, and illustrate (Figs. 7 to 10) the concentration of deformations into connections. While for the non-prestressed case connection and panel flexural deformations (most of it in the bottom connection and panel) contribute equally to top deflection (Figs. 7 and 8), panel deformations are practically negligible in the prestressed case. Assuming that all deformations concentrate into the base connection is a reasonable simplifying design assumption for prestressed walls, while it is overly conservative for non-prestressed walls. However, estimating the proportion of connection and panel deformations in design is not trivial. Figs. 7 and 8 also show that baseblock movement due to insufficiently tightened bolts contributed not unsignificantly to top deflection, particularly of course at small deflections. If this component is deducted, top deflection ductility ratios become 4,4,9,7.5,6.6 for PW1 to PW5, respectively. Converting these values for the tested 5 story specimen to the 10-story prototype yields ductility ratios of roughly 3,3,6.5,5.5,5.

Energy Dissipation Capacity Figs. 5 and 6 show the hysteresis loops at maximum displacement before failure for PW3 and PW4. If they are not particularly fat, this should not be considered as a characteristic of precast walls but rather attributed to the low reinforcement ratio in comparison with the axial load. To give a non-dimensional index for energy dissipation capacity, equivalent viscous damping ratios were calculated as follows: PW2: 14.9% (3DY), PW3: 11.7%, PW4: 7.8%, PW5: 8.2% (all 5DY). It must be noted that these values are to be interpreted and used in conjunction with the reduced secant stiffness associated with the tip of the hysteresis loop. While the prestressed walls achieved somewhat smaller ductility and damping ratios, the hystersis loops of PW3 and PW4 look surprisingly similar (Figs. 5 and 6). The comparison of the different sources contributing to energy dissipation in Figs. 9 and 10 reflects the same trend as that for top deflection (Figs. 7 and 8): A strong concentration of inelastic deformations into the connections and an almost negligible panel contribution for the prestressed walls. In hindsight, the poor bond provided by the EMT tube used as PT duct must be considered an asset that contributed to the good performance of the prestressed walls, since it allowed strains to distribute to the first anchor atop the first panel. Otherwise the PT bars might have ruptured earlier.

CONCLUSIONS

Precast walls exhibiting non-monolithic behavior can be successfully designed for earthquake-resistance provided the behavioral differences to monolithic walls are appropriately considered. In particular, the reduction in ductility resulting from concentration of deformations into connections must be considered in the selection of design force levels. Spiral confined boundary elements near critical connections proved very effective in increasing ductility. Shear design must be based on a realistic model which considers the effect of horizontal connections on the shear transfer mechanism.

ACKNOWLEDGEMENTS

The research project "Hysteretic Behavior of Precast Panel Walls" is being conducted at Lehigh University, Fritz Engineering Laboratory, and was sponsored by the National Science Foundation under Grant CEE-8206674. The author would like to thank Dywidag Systems International for generously sponsoring all post-tensioning hardware. The contributions of Cheng-Cheng Chen, Jian Jin, and George Assis in design fabrication, testing, and analysis of the specimens is gratefully acknowledged. The views expressed in this paper are those of the writer and do not necessarily reflect the position of the National Science Foundation.

REFERENCES

1. Mueller, P., "Seismic Behavior of Precast Walls", Proc., 3rd U.S. National Conference on Earthquake Engineering, Vol. II, Charleston, South Carolina, USA, 1986, pp. 1239-1249.
2. Mueller, P., "Hysteretic Behavior of Precast Panel Walls", Proc., US-Japan Seminar on Precast Concrete Construction in Seismic Zones, Vol. 1, Tokyo, Japan, 1986, pp. 127-142.
3. Mueller, P., et. al., "Hysteretic Behavior of Precast Panel Walls", Report in preparation.

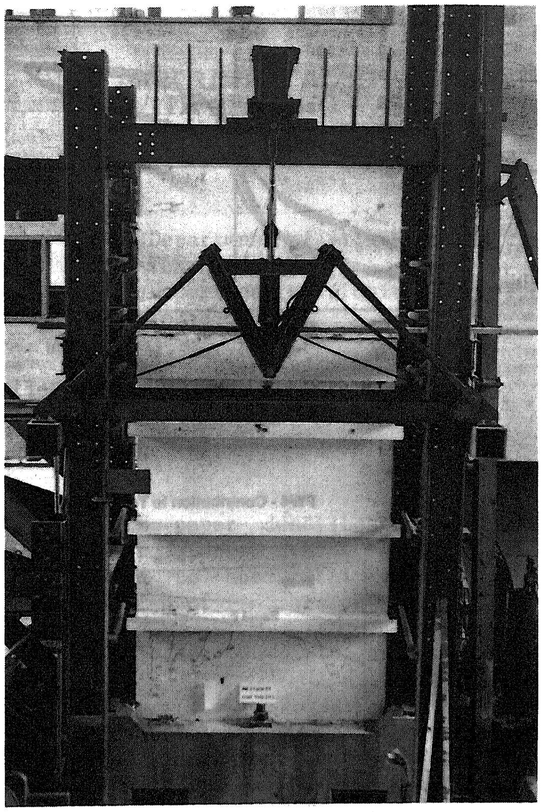

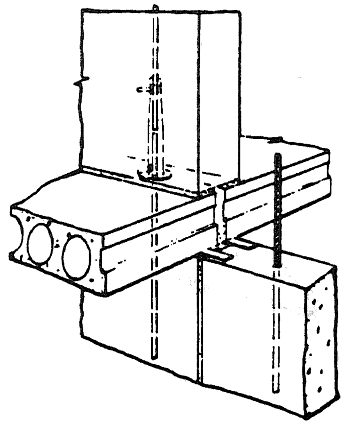

Fig. 1(b) Platform Connection

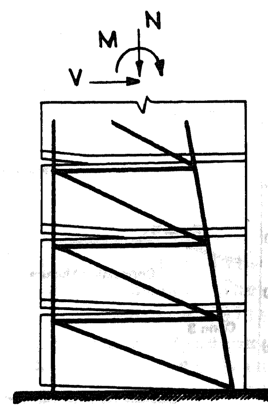

Fig. 1(a) Test Setup PW5
Cycle 27, 6 DY

Fig. 2 Truss Model for Precast Walls

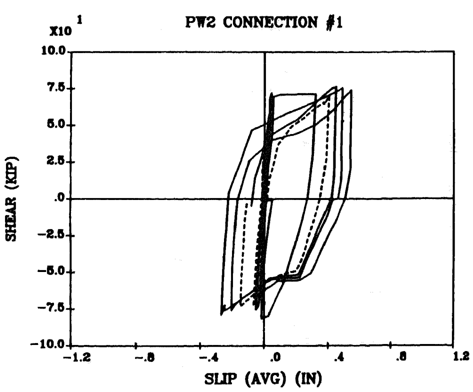

Fig. 3 Shear vs. Slip for Platform Connection

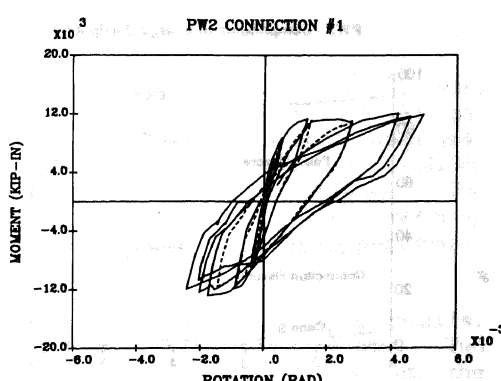

Fig. 4 Moment vs. Rotation for Platform Connection

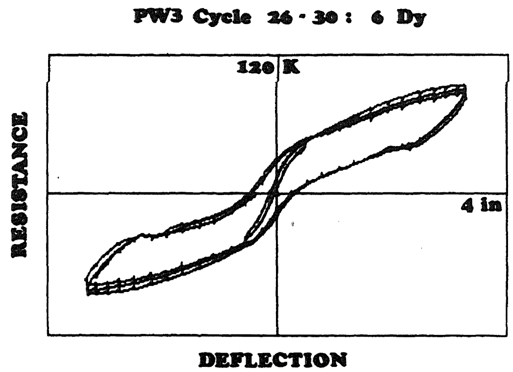

Fig. 5 Lateral Res. vs. Top Defl.
PW3 (1 in = 25.4 mm)

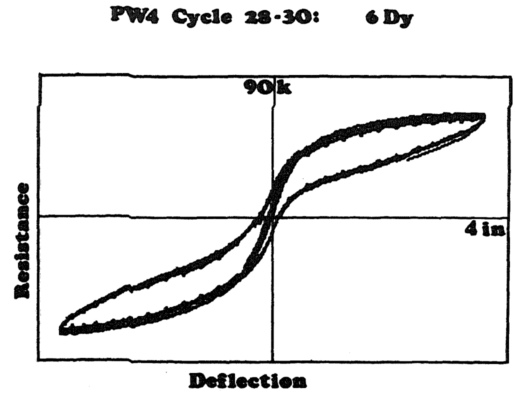

Fig. 6 Lateral Res. vs. Top Defl.
PW4 (1 kip(K) = 4.45 kN)

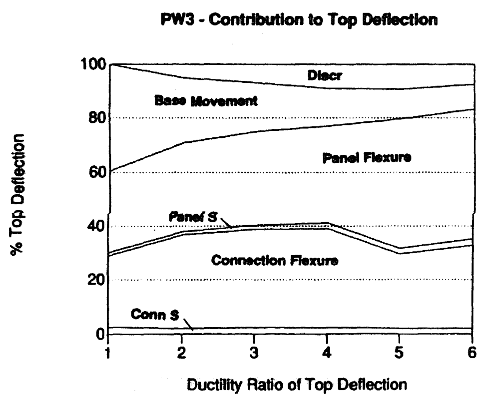

Fig. 7 Top Defl. of PW3 by
Component Contributions

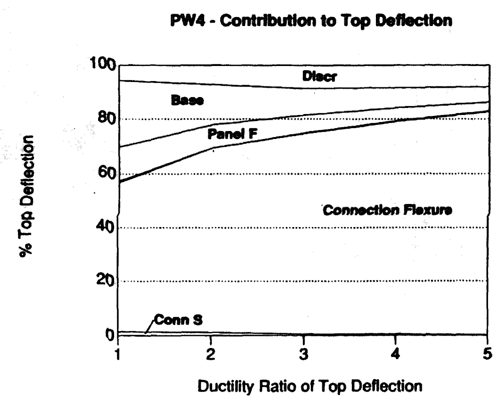

Fig. 8 Top Defl. of PW4 by
Component Contributions

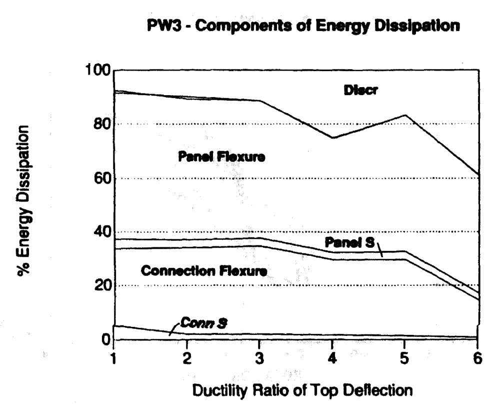

Fig. 9 Energy Diss. PW3 by
Component Contributions

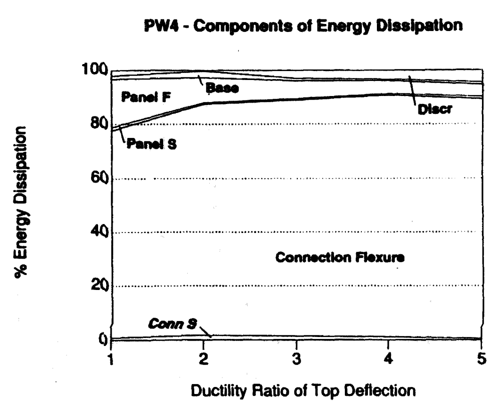

Fig 10 Energy Diss. PW4 by
Component Contributions